J Polym Res (2015) 22: 65
DOI 10.1007/s10965-015-0713-7

ORIGINAL PAPER

Novel dye-containing copolyimides: synthesis, characterization and effect of chain entanglements on developed electrospun nanofiber morphologies

Yaping Wang[1] · Ning Wang[1] · Zhuo Yu[1] · Guodong Li[1] · Xingxiang Zhang[1]

Received: 20 October 2014 / Accepted: 23 March 2015 / Published online: 1 April 2015

Abstract A series of aromatic copolyimides (coPIs) derived from pyromellitic dianhydride (PMDA) with two diamines as comonomers 4.4′-oxydianiline (ODA) and 2,6-diaminoanthraquinone (2,6-DAAQ) incorporated in variable proportions were synthesized via a conventional two-step route. The obtained copolyimides were characterized by Fourier transform infrared spectroscopy (FTIR), nuclear magnetic resonance spectroscopy (NMR), thermogravimetric analysis (TGA), dynamic mechanical analysis (DMA), scanning electron microscopy (SEM), fluorescence spectroscopy (FL) and tensile tests, etc. The flexible thin films still possessed fairly good thermal stability and high glass transition temperature (T_g), and exhibited various fluorescence intensities. All PI films exhibited excellent thermal stability without significant decomposition up to 500 °C under nitrogen atmosphere. With the increased bulky anthraquinone substituents in coPI chain, the coPIs showed much higher tensile strength and modulus (improved by 23.3 and 38.4 % respectively), and enhanced fluorescence intensities. The chain entanglements of polymer solutions with different inherent viscosities have been used to elaborate the transition from electrospraying to electrospinning in regard to the developed morphologies of electrospun membranes.

Keywords Copolyimide · Synthesis · Fluorescence · Electrospun membrane · Inherent viscosity · Chain entanglements

✉ Ning Wang
wangntjpu@hotmail.com

[1] Tianjin Municipal Key Lab of Fiber Modification and Functional Fiber, School of Material Science and Engineer, Tianjin Polytechnic University, Tianjin 300387, China

Introduction

Aromatic polyimides (PIs) are one of the most important high-temperature polymers with superior performance i.e., excellent thermo-oxidative stability, high solvent resistance, pretty good mechanical and dielectric properties under harsh circumstances [1]. Therefore, they have been successfully prepared for many applications such as insulating or dielectric materials, high temperature fibers, and advanced polymer matrix composites in microelectronics, separation, and aerospace industries [2–5]. However, full aromatic polyimides with rigid chains and strong interchain interactions originated from intra/inter chain charge transfer complex (CTC) formation and electronic polarization, often have low solubility in common organic solvents and relatively high softening temperature [4]. This issue makes the processing by conventional techniques like melt processing or solution casting either difficult or too expensive to be commercially viable. Much effort has been taken to improve their comprehensive performance, especially the solubility in organic solvents and melt processability [6–10]. Park et al. [11] and Eichstadt et al. [12] synthesized aromatic alternating copolyimides and amorphous partially aliphatic polyimides using a poly (amic acid ester) precursor through copolymerization respectively. The disruption of high symmetry and recurrence of regularity through copolymerization can impart these copolyimides better solubility [13] and various functionalities (such as electroluminescence (EL) for organic light-emitting diodes (OLED) [14] and photoluminescence (PL) for solar cells [15]). Meanwhile, functional polyimides with special photophysical properties have been successfully prepared in the past two decades [14–16]. Thelakkat et al. [15] synthesized high fluorescent copolyimides by incorporating differently substituted dye chromophore into the main chain and Kim et al. [16] reported the preparation of red electroluminescent devices by simply

dispersing the dye in the poly (ether imide) matrix. They both expected to combine the high thermal stability and chemical resistance of PI with the unique optical properties of organic dyes to obtain desired performances.

2,6-diaminoanthraquinone (2,6-DAAQ) is a commercially available and low-cost organic dye, and DAAQ has been applied to produce organic nanowire waveguide arrays and self-assembled nanowires for field emission devices [17, 18]. Yakovlev et al. [19] has synthesized colored copolyamides by introducing 2,6-DAAQ into the polyamide chain, but to our best knowledge there is no report for this type of dye-containing polyimide through copolymerization. In this paper, 2,6-DAAQ has been incorporated as the diamine comonomer into the typical two-step reaction scheme to obtain different Poly(amic acid) (PAA) precursors through copolymerization. Then, PAA solutions were thermally imidized and the resulting coPIs were characterized by Fourier transform infrared spectroscopy (FTIR), nuclear magnetic resonance spectroscopy (NMR), thermogravimetric analysis (TGA), dynamic mechanical analysis (DMA), tensile tests, scanning electron microscopy (SEM), and fluorescence spectroscopy (FL). The wavelengths and intensities of fluorescence of coPIs were varied by incorporating different amounts of the dye moiety through copolymerization. The correlation between inherent viscosities of these PAA solutions and the resulting fiber forming ability (also termed electrospinnability) was discussed in the end. The experimental results demonstrated that the high-performance copolyimides with the DAAQ chromophore unit in the main chain showed potential for optoelectronic or other functional applications.

Experimental

Materials

Pyromellitic dianhydride (PMDA, 98 %) was purchased from Sinopharm Chemical Reagent Co., Ltd, and purified via vacuum sublimation. 4,4′-oxydianiline (4,4′-ODA, 98 %) and 2,6-diaminoanthraquinone (2,6-DAAQ, 98 %) were purchased from Shanghai Reagents Company, recrystallized twice from ethanol and vacuum dried before use. *N*,*N*-dimethylacetamide (DMAc) was obtained from Tianjin Guangfu Reagents Company, distillated under reduced pressure over calcium hydride and stored over 4 Å molecular sieves prior to use.

Synthesis of PAA solutions, preparation of solution-cast films and electrospun membranes

A typical procedure of polymerization of PAA was described as follows. Powders of 4,4′-ODA and 2,6-DAAQ with a certain molar ratio were added into a dry three-neck glass flask under flowing nitrogen. After the two diamines were completely dissolved in DMAc under vigorously stirring, PMDA was gradually added in several portions. An additional part of DMAc was added to adjust the solid content to be 15 %. The reaction mixture was further stirred for 4 h in ice bath and the obtained PAA solution was sealed and kept in a freezer until use.

The scheme of synthesis shown in Fig. 1 describes the preparation of different copolymers with varying mol% of incorporated anthraquinone substituents. The molar ratios of 2,6-DAAQ to 4,4′-ODA were set to be 1:1, 1:2, 1:3 and 1:4 respectively (Table 1). The total molar amount of both diamines was equal to that of the dianhydride PMDA. These filtered and degassed solutions were cast into free-standing transparent films on dry and clean glass plates and electrospun into fiber webs using a high-voltage electrostatic spinning apparatus (Beijing Fuyouma Technology Co. Ltd), respectively. All the films and membranes were first dried at 60 °C for 12 h in an air-convection oven to remove the residual solvent. Then the tack-free films (30~50 μm thick) were transferred to a vacuum oven for thermal imidization using the following program: heating from ambient temperature to 100 °C, 100 °C to 200 °C and 200 °C to 300 °C at a rate of 2.5 °C/min and annealing each for 30 min at the three ending temperature.

Characterization

Inherent viscosities (η_{inh}) of as-polymerized PAA solutions were obtained at a concentration of 0.5 g/dL in DMAc at 30 °C using an Ubbelohde viscometer. Fourier transform infrared spectroscopy (FTIR) of the obtained films and membranes were recorded on a Bruker Vector 22 spectrometer with an attenuated total reflectance (ATR) accessory. High-resolution solution ^{1}H NMR spectra were collected on a Bruker 400 NMR spectrometer at room temperature, using DMSO-d_6 as solvent and tetramethylsilane (TMS) as internal standard. Elemental analyses were performed with an Elemental Vario EL elemental analyzer. Thermogravimetric analysis (TGA) was performed by Thermogravimetry (TG, NETZSCH STA 409 PC/PG TG-DTA) under nitrogen flow from room temperature to 800 °C at a heating rate of 10 °C/min. Dynamic mechanical analysis (DMA) of the films were carried out using Dynamic mechanical Analyzer (DMA, NETZSCH DMA 242) under tensile mode from room temperature to 450 °C at a frequency of 1Hz and heating rate of 5 °C/min. A field emission scanning electron microscope (FE-SEM, HITACHI S-4800) was used to observe the surface morphology of electrospun membranes. UV–vis absorption spectra of was measured with a UV-1901 spectrometer at room temperature. Fluorescent spectra of PI films were measured at room temperature using a fluorescence spectrophotometer (Tianjin Gangdong Tech, F-380) with an excitation wavelength of 350 nm. The samples were excited in a front-

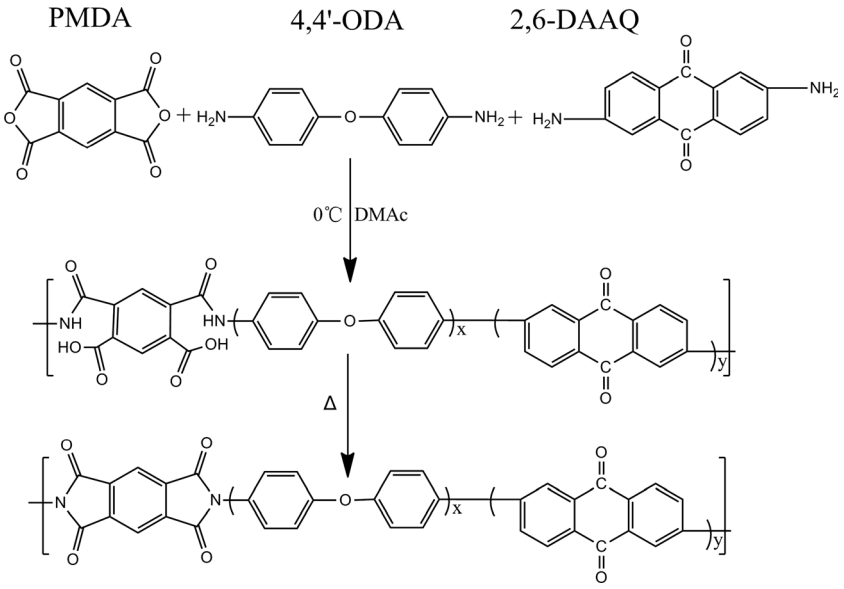

Fig. 1 Synthesis scheme of coPI films

face arrangement to minimize self-absorption. Tensile tests of films were carried out on a CMT4204 electromechanical universal testing machine (SANS) with a crosshead speed of 5 mm/min at room temperature. Samples of PI film were cut into 50 mm×10 mm strips along the film casting direction. Tensile properties reported here represented an average value at least five measurements for each yellowish-brown sample. Toughness was calculated by integrating the areas under the stress–strain curves and then dividing by the related film density around 1350 kg/m^3 [20, 21].

Results and discussion

Synthesis and characterization of coPIs

CoPIs were synthesized through the most commonly used two-step method [1–3], i.e., the reaction of an aromatic dianhydride with two comonomer diamines to obtain soluble poly (amic acid) (PAA) as a precursor, which was thermally converted to a final polyimide.

Table 1 Polymerization condition and PAA properties derived from various diamines

Copolyimide	Molar ratio of monomers			η_{inh} (PAA) (dL/g)	PAA cast film flexibility
	2,6-DAAQ	ODA	PMDA		
coPI-1	1	1	2	0.35	very brittle
coPI-2	1	2	3	0.52	very brittle
coPI-3	1	3	4	1.37	flexible
coPI-4	1	4	5	1.77	flexible
PI		1	1	1.93[a]	flexible

The structure of the polyimides were identified by FTIR, ^{1}H-NMR spectroscopy and elemental analysis. Figure 2 showed the typical FTIR spectra of coPI-4 and its poly (amic acid) precursor coPAA-4. The Imidization of films was partially proven by the disappearance of absorption band at around 1646, 1540, and 2500~3500 cm^{-1}, which can be assigned to C=O stretching vibration of secondary amide (−NHCO-), N-H stretching vibration of polymer chain end groups and O-H groups of PAA. And the characteristic absorbance bands of imide ring at about 1775, 1715, 1368 and 718 cm^{-1}, which were attributed to asymmetric/symmetric C=O stretching vibration of the imide ring, C-N stretching and C-N bending vibration, were also a further proof of complete imidization.

In order to clarify the composition of coPAA, ^{1}H-NMR spectra of a representative coPAA-4 were illustrated in Fig. 3. ^{1}H-NMR spectra of coPAA-4 showed the aromatic protons of the two diamine ODA and DAAQ moiety in PAA resonated in the region of 6.87~7.47 ppm, and the protons of the PMDA moiety appeared at a lower field of 7.55~8.20 ppm. Due to the existence of different PAA structural isomers, the observed spectra was relatively broad and the peaks were merged. Among these peaks, the ODA/DAAQ molar ratio in coPAA can be determined by comparing the peaks area in the region of 6.87~7.09 ppm with that of 7.34~7.47 ppm. The ODA/DAAQ molar ratio was calculated to be approximate 3:1, which was in good agreement with the chemical structure of coPAA-4. Furthermore, results of elemental analysis for coPI-4 was summarized as follows: Anal. Calcd for coPI-4 (x:y=4:1): C, 67.54; N, 7.04; O, 22.5; H, 2.92. Found: C, 67.51; N, 6.96; O, 23.0; H, 2.53. Consequently, all the above results supported the formulated chemical structure of copolymers.

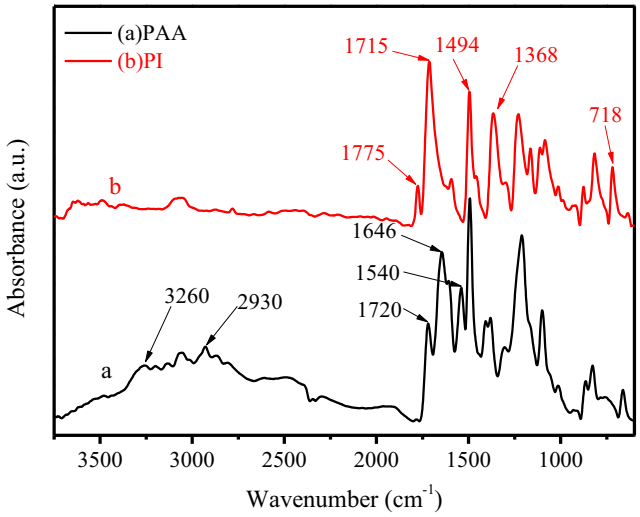

Fig. 2 FTIR spectra of coPI-4 and coPAA-4

As shown in Table 1, there was a direct relationship between the values of inherent viscosity (η_{inh}) and the incorporated molar amount of DAAQ. Copolycondensation of DAAQ and ODA was seen to result in the formation of copolymers with lower values of η_{inh} compared with the homopolymer (with the exception of DAAQ). For the synthesis of copolyimide precursors, DAAQ with lower nucleophilicity (pK_1=0.73 and pK_2=−1.00) displayed correspondingly lower reactivities than ODA (pK_1=5.20 and pK_2=4.02) in the copolycondensation process [2, 19, 22]. Practically, the polymerizability of the dianhydride with diamine was always discussed on the basis of the η_{inh} values of the obtained PAA. And the η_{inh} value of PAAs was closely related to molecular weight and film flexibility of final PI. Thus the relatively low

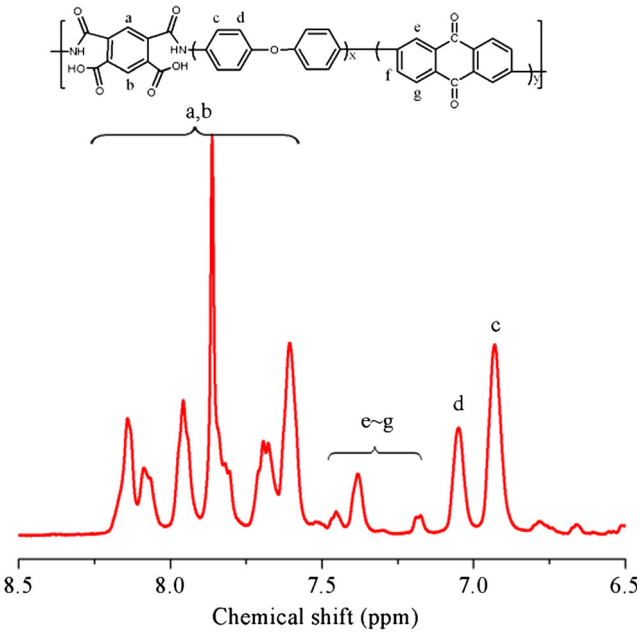

Fig. 3 ^{1}H-NMR spectra of coPAA-4

η_{inh} or molecular weight of the coPIs might be attributed to the lower chain entanglement of PMDA-DAAQ oligomeric block stemmed from the less reactive diamine DAAQ [22–24]. As the DAAQ amount in the initial reacting mixture increased, the molecular weight of the copolyimides decreased monotonously. Precursors of coPI-1 and coPI-2 with relatively low inherent viscosities (η_{inh}=0.35 and 0.52), showed unsatisfactory film-forming ability probably owing to their too low molecular weights. To obtain films with certain flexibility and toughness, optimum polymerization conditions were chosen and characterization of the suitable films coPI-3 and coPI-4 was carried out later.

Thermal properties of coPIs

Thermal properties are important for PIs since they are potentially used as heat-resistant materials. The thermal stability of coPIs was measured by TGA in nitrogen flow, as shown in Fig. 4. All the three films exhibited excellent thermal stability without significant decomposition up to 500 °C under nitrogen atmosphere and remained more than 56 % char yield at 800 °C. In comparison with the homopolymer, the two flexible coPI films showed nearly the same but slightly low decomposition temperature at 5 % weight loss (T_d^5). This can be ascribed to the thermal degradation of low molecular weight PMDA-DAAQ oligomeric block at relatively low temperature [25, 26]. Nevertheless, the TGA data indicated that they still possessed fairly high thermal stability with the introduction of bulky anthraquinonyl groups in the backbone. It's especially preferable for application like LED devices under high-temperature operation.

DMA was used to characterize the dynamic thermal mechanical property of coPI films. Figure 5 showed the plots of storage modulus (E') and tan δ as a function of temperature. The value of T_g was determined from the peak temperature of the tan δ value. As displayed in Table 2, the T_g of PI films

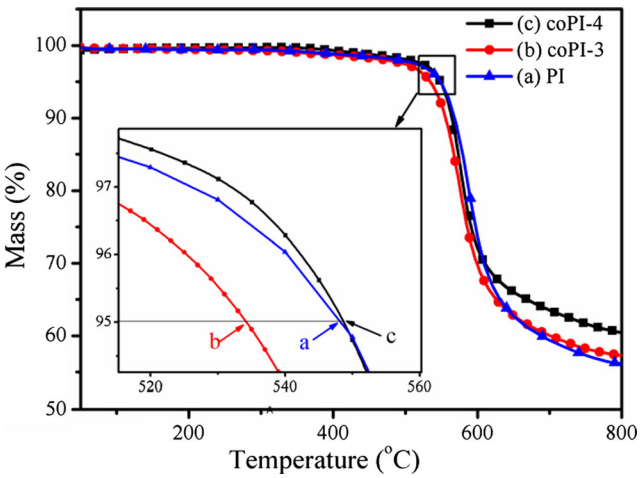

Fig. 4 TGA curves of PI films under N_2 atm

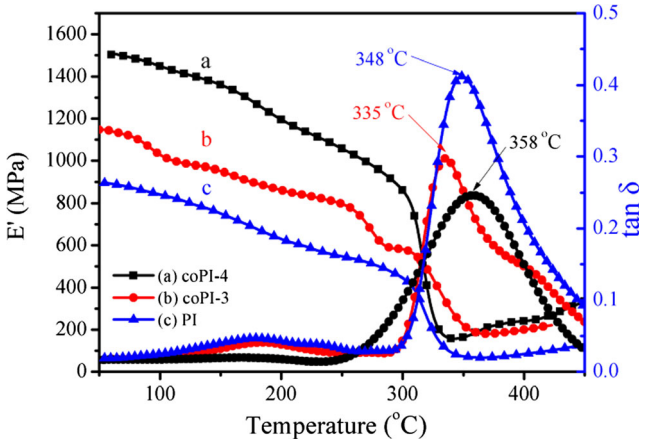

Fig. 5 Dynamic storage modulus and tan δ changes of the PI films under tension mode

ranged from 335 to 358 °C with different molar ratio of the two diamines. One notices that even though coPIs had higher initial storage modulus at room temperature, they showed less dynamic thermomechanical stability when referred to T_g. It can be explained by the higher stiffness but less restricted mobility of coPI chain. And the change of the storage modulus ($\Delta E'$) with the temperature range from room temperature to the corresponding T_g, was smaller for PMDA-ODA based PI as compared to coPIs. This trend was expected since the coPIs are not quite as linear and possess as compact chain stacking as PMDA-ODA based PI. Meanwhile, as mentioned before, the mobility of low molecular weight PMDA-DAAQ oligomeric block in the backbone can be better than the well-packed PMDA-ODA chain, which will be accelerated when the temperature was beyond the glass transition region [27].

Optical properties of coPIs

According to previous reports [28, 29], aromatic polyimides themselves usually demonstrate weak but distinct fluorescence spectra due to the formation of charge transfer (CT) complexes. And increased molecular aggregation or denser packing of the polymer chains lead to a significant increase in the CT fluorescence intensity. The spectral characteristics

Table 2 Thermal properties of coPI and PMDA-ODA PI films

Sample	T_d^5 (°C)[a]	E_i'(GPa)[b]	T_g (°C)	$\Delta E'$ (GPa)[c]
PI	548	1.14	358	0.95
coPI-3	535	1.50	335	1.33
coPI-4	549	0.89	348	0.82

[a] T_d^5 is the decomposition temperature at which 5 % weight loss is detected

[b] E_i' is the initial storage modulus value at room temperature under the described DMA condition

[c] $\Delta E'$ denotes the storage modulus decrease from room temperature to the corresponding T_g

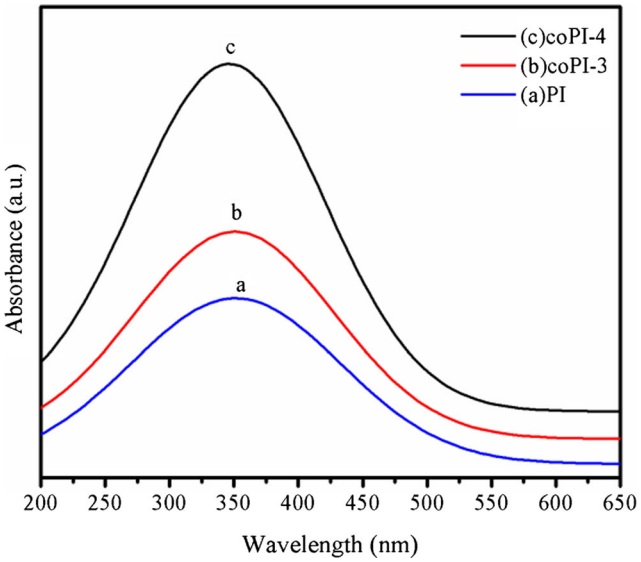

Fig. 6 UV–Vis absorption spectra of PI films on quartz plates

such as the optical absorption and fluorescence emission of DAAQ in different dilute solvents have been investigated already, but the solid-state fluorescence of coPI thin films can be varied due to molecular aggregation and interaction of DAAQ chromophore units.

The optical properties of the resulting novel coPI films were investigated by UV–vis absorption spectra and fluorescence emission spectra at room temperature. Figure 6 illustrated the UV–Vis absorption spectra of PI films on quartz plates. There was no distinct shift in absorption maximum (around 350 nm) between the coPI films, indicating the absence of significant DAAQ chromophore aggregation in the solid-state films. And the absorption maximum at 350 nm was due to the characteristic π-π* transition of anthraquinone groups in DAAQ, as well as the charge-transfer interaction of the imide groups. The absorption intensity at 350 nm increased with more incorporated DAAQ groups in the

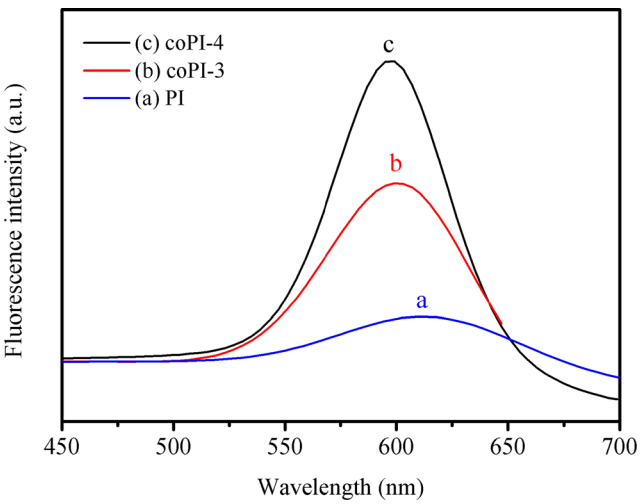

Fig. 7 Fluorescence emission spectra excited at 350 nm for PI films

copolymer chain, proving that the DAAQ dye was in fact incorporated into polymer main chain and that the absorption energy varied with the amount of incorporated DAAQ groups. This fact enables us to tune the absorption as well as fluorescence emission in such polymers.

Figure 7 showed the fluorescence emission spectra at 350 nm excitation for the PI thin films with average thickness of 10 μm. The intensity of fluorescence emission in solid film state as well as its dependence on the amount of incorporated DAAQ was studied. And the fluorescence quantum yields in the solid state were determined using a calibrated integrating sphere. The PI films exhibited broad and structureless fluorescent properties. And the PMDA-ODA homopolymer showed longer maximum wavelength (λ_{max}=610 nm) but weaker intensity of emission spectra than the coPIs (λ_{max}=588~589 nm). The phenomenon could be explained by the fact that the more the electron-accepting ability of the imide moiety and the electron-donating ability of the amine in the PIs increased, the more the emission spectra appeared in a longer wavelength range [28].

Fluorescence emission with a λ_{max} at about 590 nm was observed for all the coPI films and the intensity of λ_{max} increases moderately with increase in amount of DAAQ in the polymer chain. To be mentioned here that the variation in fluorescence intensity of coPIs was not as great as we have estimated, according to the amount of different incorporated DAAQ chromophore fragments in the copolyimide. This suggests that introduction of DAAQ moieties as comonomer augments the charge transfer properties, and high content of DAAQ chromophore leads to some fluorescence quenching through aggregation in solid state [30]. Moreover, in the case of solid film state the fluorescence quantum yields of the copolyimides can reach to 40 % for coPI-4 and 34 % for coPI-3 respectively, which were greatly enhanced compared with that of the PMDA-ODA homopolymer (8 %). This phenomenon could be attributed to the unique electron transition and energy conversion characteristics of DAAQ groups in the copolymer main chain and the easier release of the excited-state energy for copolyimides owing to their greater conformational mobility. As UV–vis absorption spectra and fluorescence emission spectra illustrated, it can be concluded that the coPIs with relatively high photoluminescence efficiency were promising high temperature resistant polymers for organic photoluminescent and photoelectric applications.

Tensile properties of coPIs

Representative stress–strain curves for tensile tests of PI films were depicted in Fig. 8. The tensile properties such as tensile modulus (E), tensile strength (σ_b), and elongation at break (ε_b) can to some extent reflect the backbone's stiffness/linearity, chain steric structure and entanglement. As shown in Table 3, the coPI films exhibited higher tensile strength and tensile modulus but smaller strain at break than homopolymer PI. It is not unusual since rigid polymers are in general stronger than flexible polymers. In particular, σ_b and E of the coPI films were gradually increased with incorporation of more molar ratio of bulky anthraquinonyl groups, which were increased by 23.3 and 38.4 % respectively. And for PMDA-ODA based PI, with more flexible ether linkage of the ODA moiety in the backbone and higher degree of chain entanglement, it showed greater ε_b and toughness.

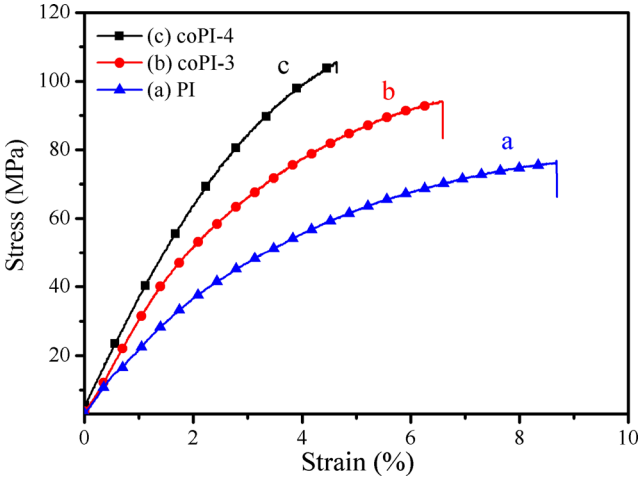

Fig. 8 Typical stress–strain curves of PI films

Electrospinning of nanofiber membranes and the correlation between η_{inh} and the electrospinnability

Electrospinning has emerged as a new technique for obtaining various functional nanofibers owing to the advantages of low cost, flexible operation conditions, and a continuous production process. The procedure probably leads to different electrospun morphologies with more extended chain conformation under electrical field according to the properties of various polymer solution. And it may also result in more molecular chain orientation and alignment than the solution-cast films. In the paper, the electrospun samples showed different morphologies to the corresponding polymer solutions with distinct extent of chain entanglements. It could also be a good

Table 3 Tensile properties of coPI and PMDA-ODA PI films

Sample	σ_b (MPa)[a]	E (GPa)[b]	ε_b (%)[c]	Toughness (kJ/kg)
PI	76.3	2.32	8.7	3.4
coPI-3	94.1	2.56	6.6	3.1
coPI-4	105.6	3.14	4.7	2.3

[a] Tensile strength

[b] Tensile modulus

[c] Elongation at break

reflection of the inherent viscosity data shown in Table 1, and be in consistent with theoretical analysis based on chain entanglement of the dilute solution.

The electrospinning process was conducted using a syringe with a spinneret having a hole diameter of 0.8 mm at a applied voltage of 25 kV at 50 °C. Different PAA solutions with the same 10 % solid content were extruded through the spinneret at a constant feeding rate of 1.250 mL/h and the distance between the spinneret and plate collector covered with aluminum foil was set to be 20 cm.

With the increase of molar ratio of flexible ODA, the developed morphologies changed from beaded microspheres, beads with incipient fibers to beaded fibers and bead-free fibers (Fig. 9a to d). All the electrosprayed microspheres had average diameters ranging from 1~3 μm. There were a few filaments adhering to the surface of microspheres which resulted from the stretching deformation of PAA under electrostatic field. And the microspheres remained smooth and compact without much deformation or collapse even after thermal imidization. The bead-free fiber diameters were in the range of 100–150 nm.

According to the previous studies [31–33], the electrospinning process with developed morphology can be greatly influenced by the properties of the polymer solution such as viscosity of the solution and the amount of chain entanglements. Viscosity is a function of the concentration of solution and the molecular weight of the polymer. In view of the parameter chosen in our experiments, the determination of the three concentration regime (semidilute unentangled, semidilute entangled, and concentrated regime) [31, 32] for coPIs was analyzed by the dependence of inherent viscosity (η_{inh}) (Table 1) on the molecular weight of the polymer.

In the case of dilute concentration regime (η_{inh}=0.35~0.52 dL/g), where the polymer chains are distributed randomly as separate spheres (Fig. 9a and b), separated chains behave independently and the polymer molecules mainly interact with the solvent molecules. In the semidilute range, the transition from dilute to unentangled and unentangled to entangled domain, was observed by the change of inherent viscosity from 0.52 to 1.37 and 1.37 to 1.77 dL/g. When in the semidilute unentangled regime, the solution viscosity is controlled by the intramolecular excluded volume effects. While above the critical inherent viscosity of chain entanglements, the intermolecular entanglements have dominating effect on the rheology of the solution, resulting in the formation of beaded fibers (Fig. 9c). In the case of studied polymer solution with η_{inh}=1.77 dL/g, the extent of the chain entanglement was great enough to produce bead-free fiber (Fig. 9d). The results derived from the SEM micrographs are consistent with data obtained by viscosity measurements. It revealed that the amount of chain entanglements is one of the main factors that influence the fiber morphology.

Although the novel copolyimides could be utilized to produce efficient luminescent materials, the nanofiber mats prepared by electrospinning method were not strong or uniform enough to fabricate the related functional devices for applications like optoelectronic conversion, membrane separation or metal ion sensing. Therefor, as the next step of the present work, we will carry out further improvement of the properties of electrospun nanofiber and pay more attention to their practical applications.

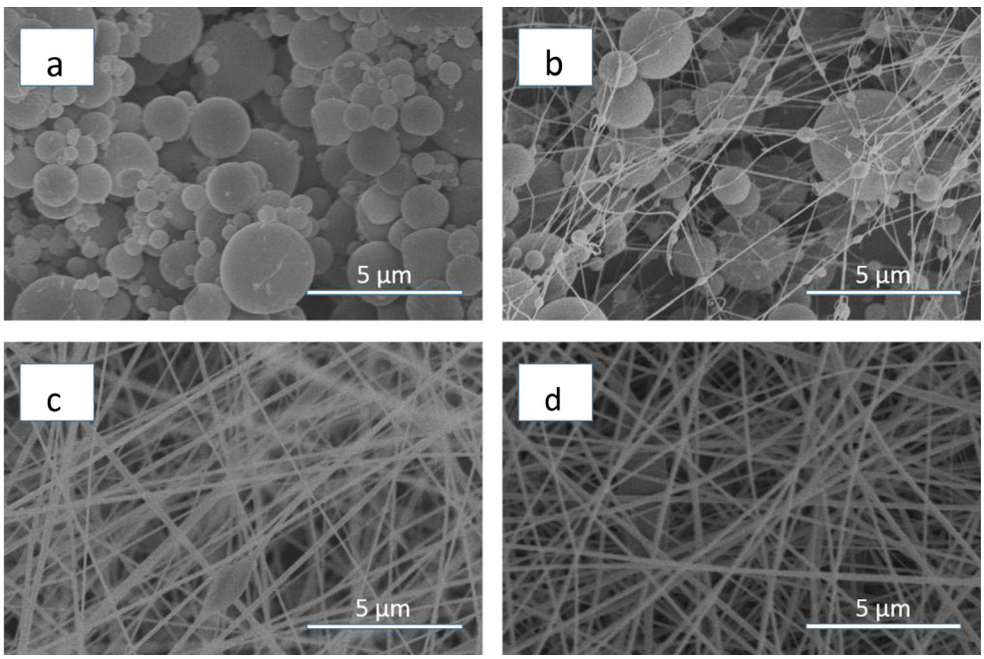

Fig. 9 SEM images of the electrospun coPI memebranes morphology with various diamine molar ratio: (**a**) coPI-1; (**b**) coPI-2; (**c**) coPI-3; (**d**) coPI-4

Conclusions

A novel class of dye-containing copolyimides were synthesized via the polycondensation reactions of two diamine comonomers 2,6-DAAQ and ODA with the aromatic dianhydride PMDA in this study. Flexible films and electrospun membranes with varying molar ratio of diamines was obtained by conventional solution casting and electrostatic electrospinning technique after thermal imidization. Strong solid-state fluorescence in coPIs was obtained by incorporating different substituted DAAQ chromophore core into the polymer main chain. They showed high thermal stability, enhanced tensile modulus and strength as compared to homopolymer PI. The backbone's stiffness/linearity, chain steric structure and entanglement have a major effect on above macroscopic properties. The developed morphology of electrospun membranes with different inherent viscosities, can change from beaded microspheres, beads with incipient fibers to beaded fibers and bead-free fibers. The results showed that the amount of chain entanglements is one of the main factors that influence the fiber morphology. Considering the effective photoluminescence of DAAQ and the distinctive mechanical properties, high thermal stability, and chemical resistance of PI, these thin films and electrospun membranes might find potential applications in OLED, thin-layer solar cells, etc.

References

1. Ghosh MK, Mittal KL (eds) (1996) Polyimides: fundamentals and applications. Marcel Dekker, New York
2. Volksen W (1994) High Perform Polym 117:111–164
3. Liaw DJ, Wang KL, Huang YC, Lee KR, Lai JY, Ha CS (2012) Prog Polym Sci 37:907–974
4. Ding M (2007) Prog Polym Sci 32:623–668
5. Zhuang YB, Gu Y (2013) J Polym Res 20:168
6. Liaw DJ, Liaw BY, Li LJ, Sillion B, Mercier R, Thiria R, Sekiguchi H (1998) Chem Mater 10:734–739
7. Chisca S, Musteata VE, Stoica I, Sava I, Bruma M (2013) J Polym Res 20:111
8. Li F, Ge JJ, Honigfort PS, Fang S, Chen JC, Harris FW, Cheng SZ (1999) Polymer 40:4987–5002
9. Li Y, Wang Z, Li G, Ding M, Yan J (2012) J Polym Res 19:9772
10. Thiruvasagam P (2012) J Polym Res 19:9965
11. Park JW, Lee M, Lee MH, Liu JW, Kim SD, Chang JY, Rhee SB (1994) Macromolecules 27:3459–3463
12. Eichstadt AE, Ward TC, Bagwell MD, Farr IV, Dunson DL, McGrath JE (2002) Macromolecules 35:7561–7568
13. Dixit BC, Dixit RB, Desai DJ (2010) J Polym Res 17:481–488
14. Hsu SC, Whang WT, Chen SC (2003) J Polym Res 10:7–12
15. Thelakkat M, Pösch P, Schmidt HW (2001) Macromolecules 34: 7441–7447
16. Kim Y, Lee JG, Choi DK, Jung YY, Park B, Keum JH, Ha CS (1997) Synth Met 91:329–330
17. Zhao YS, Zhan P, Kim J, Sun C, Huang J (2010) ACS Nano 4: 1630–1636
18. Huang KJ, Hsiao YS, Whang WT (2011) Org Electron 12:686–693
19. Yakovlev YY, Nurmukhamedov RN, Barashkov NN, Klimenko VG, Kuzmin NI, Khabarova KG (1992) Polym Degrad Stab 37: 115–124
20. Shah D, Maiti P, Jiang DD, Batt CA, Giannelis EP (2005) Adv Mater 17:525–528
21. Jia X, Zhang Q, Zhao MQ, Xu GH, Huang JQ, Qian W, Lu Y, Wei F (2012) J Mater Chem 22:7050–7056
22. Bell VL, Stump BL, Gager H (1976) J Polym Sci Polym Chem 14: 2275–2291
23. Mazoniene E, Bendoraitiene J, Peciulyte L, Diliunas S, Zemaitaitis A (2006) Prog Solid State Chem 34:201–211
24. Bacosca I, Bruma M, Koepnick T, Schulz B (2013) J Polym Res 20:53
25. Cristea M, Ionita D, Hulubei C, Timpu D, Popovici D, Simionescu BC (2011) Polymer 52:1820–1828
26. Goeschel U, Lee H, Yoon DY, Siemens RL, Smith BA, Volksen W (1994) Colloid Polym Sci 272:1388–1395
27. Hasegawa M, Hirano D, Fujii M, Haga M, Takezawa E, Yamaguchi S, Ishikawa A, Kagayama T (2013) J Polym Sci Polym Chem 51: 575–592
28. Hasegawa M, Mita I, Kochi M, Yokota R (1989) J Polym Sci Polym Lett 27:263–269
29. Hasegawa M, Kochi M, Mita I, Yokota R (1989) Eur Polym J 25: 349–354
30. Pal H, Palit DK, Mukherjee T, Mittal JP (1990) Chem Phys Lett 173:354–359
31. Shenoy SL, Bates WD, Frisch HL, Wnek GE (2005) Polymer 46: 3372–3384
32. Chisca S, Barzic AI, Sava I, Olaru N, Bruma M (2012) J Phys Chem B 116:9082–9088
33. McKee MG, Wilkes GL, Colby RH, Long TE (2004) Macromolecules 37:1760–1767